

Characterization of carbon nanotubes by Raman spectroscopy

S. COSTA, E. BOROWIAK-PALEN*, M. KRUSZYŃSKA,
A. BACHMATIUK, R. J. KALEŃCZUK

Centre of Knowledge Based Nanomaterials and Technologies, Institute of Chemical and Environment
Engineering, Szczecin University of Technology, ul. Pułaskiego 10, 70-310 Szczecin, Poland

Application of Raman spectroscopy to analyse carbon nanotubes has been presented. Having a mixture of various carbon nanotube samples, one can easily distinguish, in a quick experiment, presence of singlewalled, doublewalled and multiwalled carbon nanotubes (SWCNT, DWCNT, MWCNT, respectively). The so-called G-line is a characteristic feature of the graphitic layers and corresponds to the tangential vibration of carbon atoms. Another characteristic mode is a typical sign of defective graphitic structures (D-line). A comparison of the intensity ratios of these two peaks gives a measure of the quality of the bulk samples. In addition, there is a third mode, named the radial breathing mode (RBM) which is very sensitive to the diameter of SWCNT and DWCNT. Additional option is application of Raman microscopy for mapping analysis and depth profiling to view the changes of intensity in various directions in the sample.

Key words: *Raman spectra; Raman mapping; carbon nanotubes*

1. Introduction

Carbon nanotubes (CNT) since their discovery became an important scientific objects of extensive research due to their interesting physical properties and technological applications. CNT have proven to be a unique system to study Raman spectra in one-dimensional (1D) systems [1, 2], and at the same time Raman spectroscopy has provided an exceedingly powerful tool to study vibrational properties and electronic structures of CNT [3, 4], particularly for characterization of CNT's diameters, and quality of the samples [5, 6]. Various carbon materials can be analysed by the Raman spectroscopy including singlewalled (SWCNT), doublewalled (DWCNT) and multi-

*Corresponding author: email: eborowiak@ps.pl

walled (MWCNT) carbon nanotubes but, unfortunately, quantitative determination of each type is impossible at present [7].

1.1. Features of Raman spectroscopy. SWCNT and DWCNT

The Raman spectra present different features being all sensitive to chiral indices (n,m) specifying the perimeter vector (chiral vector), such as the radial breathing mode (RBM) where all the carbon atoms are moving in-phase in the radial direction, the G-band where neighbouring atoms are moving in opposite directions along the surface of the tube as in 2D graphite, the dispersive disorder induced D-band and its second-order related harmonic G'-band. From these four features, the RBM is the one which appears more sensitive to the nanotube diameter (d_t) [8], according to the expression

$$\omega_{RBM} = \frac{A}{d_t} + B \quad (1)$$

where ω is the vibration frequency, and A and B are constants and vary between individual tubes and bundle tubes [1, 9]. Some authors consider only the constant A in determination of the diameter [6, 10, 11].

A DWCNT can be considered to be a kind of MWCNT for which the interlayer interaction is generally considered to be turbostratic between the inner and outer nanotubes. For armchair–armchair DWCNT, some commensurate structure can be expected and the splitting of the G'-band which is observed in 3D graphite could be seen. Another novel direction for future exploration is a small RBM linewidth (down to 0.25 cm^{-1}) occurring for the inner wall tube within an isolated DWCNT [1].

By measuring RBM for many laser energies, the diameter distribution of the nanotubes in a particular SWCNT bundle can be found [11]. The G-band is thus an intrinsic feature of a carbon nanotube closely related to vibrations in all sp^2 carbon materials. The most important aspect of the G-band is the characteristic Raman lineshape which depends on whether the nanotube is semiconducting or metallic, allowing readily distinguishing between both types. This band shows two components, the lower frequency component associated with vibrations along the circumferential direction, (G^-), and the higher frequency component, (G^+), attributed to vibrations along G direction of the nanotube axis. Previous studies show that the former component is dependent on the diameter of a nanotube while the latter does not exhibit this dependence in both, metallic and semiconducting nanotubes [10]. The D-band and G'-band features are both observed in the Raman spectra of semiconducting and metallic SWCNT at a single nanotube level. The D-band in graphite involves scattering from a defect which breaks the basic symmetry of the graphene sheet. It is observed in sp^2 carbons containing porous, impurities or other symmetry-breaking defects. On the other hand, the second-order G'-band does not require an elastic defect-related scattering process, and

is observable for defect-free sp^2 carbons. These bands show a dependence on the chirality and diameter of nanotubes [1] and on laser excitation energy [12].

The analysis of all resonance Raman effects has been greatly facilitated by introduction of the Kataura plot of the interband transitions, E_{ii} as a function of d_t for all values of (n,m) showing that each pair of indices in a nanotube has a unique set of E_{ii} transition energies, which is physically due to the trigonal warping effect of the constant energy contours for a graphite sheet [11].

1.2. Multiwalled carbon nanotubes

Multiwalled carbon nanotubes are made of concentric graphene sheets rolled in a cylindrical form with diameters of tens of nanometers [13]. Due to a large diameter of the outer tubes for typical MWCNT and because they contain an ensemble of carbon nanotubes with diameters ranging from small to very large, most of the characteristic differences that distinguish the Raman spectra in SWCNT from the spectra for graphite are not so evident in MWCNT. For example, the RBM Raman feature associated with a small diameter inner tube (less than 2 nm) can sometimes be observed when a good resonance condition is established, but this is not the usual result, since the RBM signal from large diameter tubes is usually too weak to be observable and the ensemble average of inner tube diameter broadens the signal [1].

Whereas the $G^+ - G^-$ splitting is large for small diameter SWCNT tubes, the corresponding splitting of the G band in MWCNT is both small in intensity and smeared out due to the effect of the diameter distribution within the individual MWCNT, and because of the variation between different tubes in an ensemble of MWCNT in typical experimental samples. Therefore the G -band feature predominantly exhibits a weakly asymmetric characteristic lineshape, with a peak appearing close to the graphite frequency. The most effective influence of radiation is expected in the case of the electron irradiation of MWCNT. The feature is explained by a possible appearance of radiation defects whose presence contributes to the degradation of the nanotubes but seems to be also due to broken bonds appearing during creation of vacancies [14].

In the paper, we present a simple way of evaluation of various physical properties of SWCNT from Raman spectroscopy data.

2. Experimental

The synthesis of SWCNT was described elsewhere [15]. The Raman spectra were collected using a micro-Raman Renishaw spectrometer equipped with a CCD detector. Two laser lines were used to excite the samples, 514 nm (green laser) and 785 nm (red laser). Depth profiles and mapping of selected areas were also obtained with the Raman spectrometer. All the measurements were performed at room temperature.

3. Results and discussion

3.1. Comparison between green and red lasers

The responses for excitation with different lasers revealed very rich spectra, strongly differing for each sample [16–18]. Figure 1a presents two examples, one for excitation with the green laser (514 nm) and the other for excitation with the red laser (785 nm). The resonance scattering caused by different lasers gives us information about different excitation levels as shown in the Kataura plot (Fig. 2).

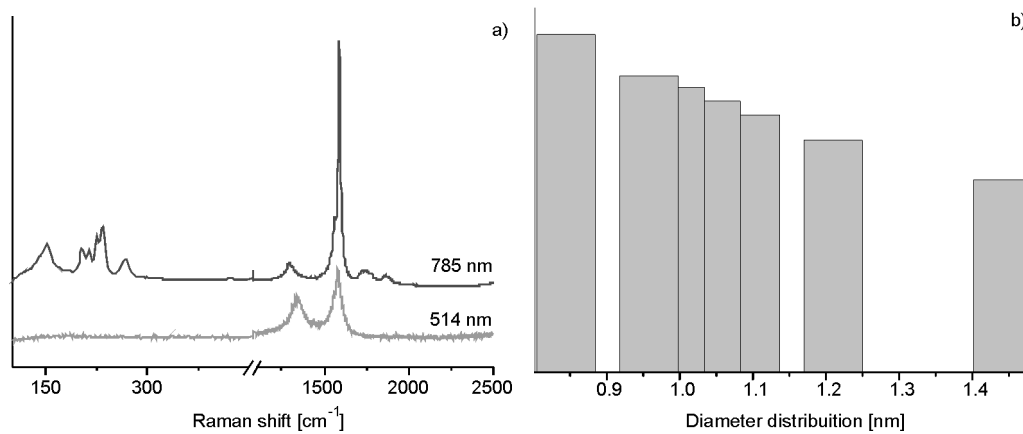
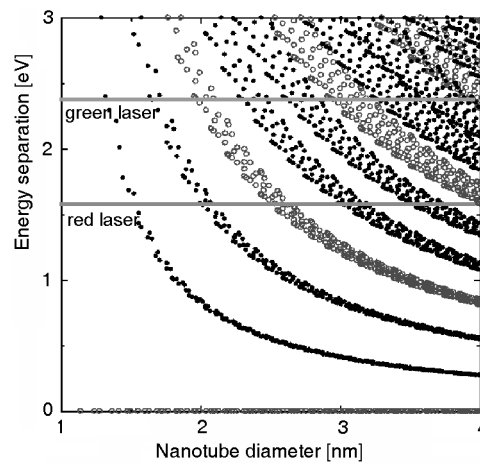


Fig. 1. Raman spectra of SWCNT excited with red (785 nm) and green (514 nm) laser radiations (a), and their diameter distribution (b)

Fig. 2. Kataura plot showing various resonance excitations as functions of various laser energies and nanotube diameters: full circles – semiconducting tubes, open circles – metallic tubes ($\gamma = 2.9$ eV, $a_{cc} = 0.144$ nm)



In the same figure, the radiation energies of the lasers used in our measurements are marked. In order to gain more information about the type of excited nanotubes, it is necessary to calculate the diameter distribution, using data from the red laser, since

the RBM with green laser is not clear. Also the intensity of *G* band increases when we use the 785 nm laser.

3.2. Determination of diameter distribution

Four characteristic features of a SWCNT sample may be found in Raman spectra presented in Fig. 1a. An RBM band is visible in the red laser spectra. For typical SWCNT bundles of the diameter $d_t = 1.5 \pm 0.2$ nm, $A = 234 \text{ cm}^{-1} \cdot \text{nm}$ and $B = 10 \text{ cm}^{-1}$ have been calculated [1]; B is an upshift in ω_{RBM} due to tube–tube interactions. The calculated diameter distribution was obtained using Eq. (1) (Table 1, Fig. 1b). The range of diameters varies between 0.8 nm and 1.5 nm. According to the Kataura plot, with the red laser we only obtain signals from semiconducting tubes but the green laser shows that we also have metallic tubes. These facts indicate how the analysis with lasers of various energies is important, because each experiment can give different data on optical and physical properties. The analysis of RBM band also allows one to distinguish between SWCNT, DWCNT and MWCNT. Figure 3a shows different RBM bands in different nanotubes. DWCNT spectrum presents a double RBM due to the diameters of the inner and outer tubes. According to Eq. (1), the band of higher Raman shift corresponds to the inner diameter and the one with lower Raman shift to the outer diameter.

Table 1. Diameter distribution calculated from the RBM feature using Eq. (1)

Raman shift [cm^{-1}]	Diameter [nm]
152.275	1.441997
183.419	1.209809
203.352	1.096779
214.397	1.042795
225.421	0.993964
234.225	0.958133
267.121	0.844396

3.3. D band–G band relation

The ratio of the intensities of D and G bands is a good indicator of the quality of bulk samples. Similar intensities of these bands indicate a high quantity of structural defects. Figure 3b presents these bands in various kinds of nanotubes. MWCNT spectrum is the one which shows the lowest ratio, consequently higher quantity of structural defects due to its multiple graphite layers. Both SWCNT and DWCNT show higher differences in intensities of D and G bands.

The ratio between D and G band and the RBM and its relation to the diameter distribution are very important factors allowing one to distinguish between three types of nanotubes with a single analysis.

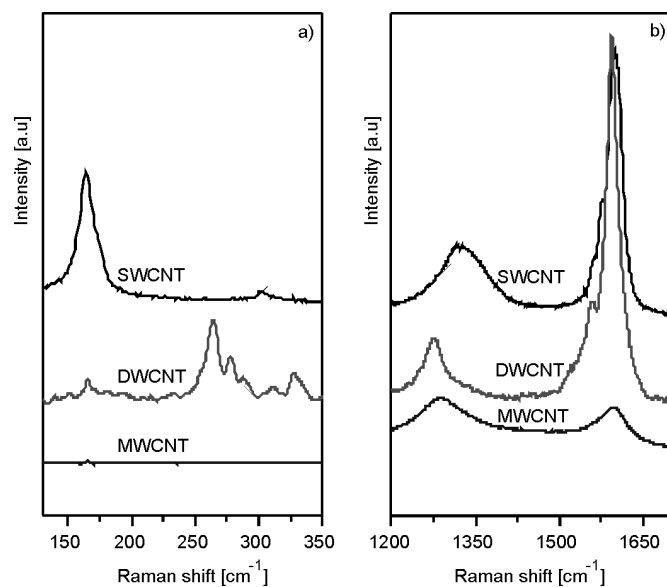


Fig. 3. Raman spectra of SWCNT, DWCNT and MWCNT:
a) RBM, b) D and G bands (laser excitation 785 nm)

3.4. Mapping

The energy of the first electron transition between semiconducting SWNTs is usually too small to be observed with standard Raman spectroscopy setups. However

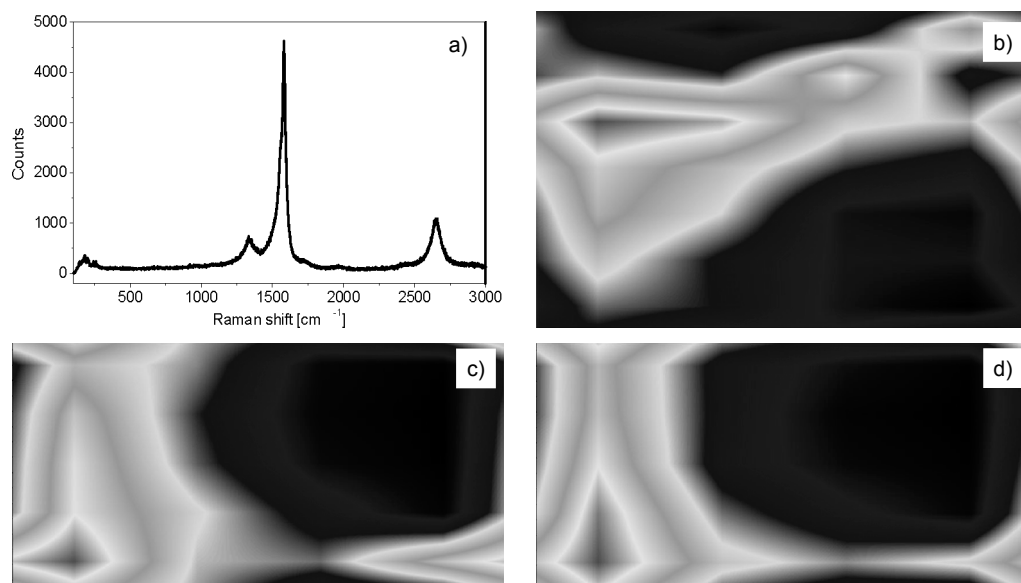


Fig. 4. Raman spectra of a CNT sample (a), and Raman two dimensional map images of RBM (b), G (c), and D (d) bands. Laser excitation 785 nm



Fig. 5. Raman mapping of RBM band. Comparison between a top view (left panel) and a 3D view (right panel). The grayscale indicates the intensities of the band. Laser excitation 785 nm

it is possible to observe it in a convenient range in a multidimensional map [1]. A map of each feature can be obtained with this technique. The mapping allows one to observe the homogeneity of the sample by screening a larger area as in the case of a standard Raman microscope measurement [19]. Figure 4 presents a mapping image of three most important features in Raman spectrum, and its distribution in the area of the analyzed sample. The mapping spectra can be visualized in two or three dimensions with similar results such as the images presented in Fig. 5.

3.5. Depth profile

With the technique described in the paper it is also possible to analyse the Raman response as a function of the depth of the sample. The depth profile of *G*-band of SWCNT is shown in Fig. 6 and it allows choosing the area of the sample which would give the highest intensity of the Raman signal. In the present case, one can conclude that the best signal is obtained at 1 μm depth in the sample. The depth profile can also be visualized in two or three dimensions.

4. Conclusions

Raman spectroscopy is a powerful technique with various options such as area mapping, depth profile for beyond the standard spectra analysis. The energy of laser excitation is also very important due to the results obtained, as shown in the Kataura plot. One can also easily determine the presence of different types of carbon nanotubes in the analyzed sample including determination of the diameter in the case of SWCNT and MWCNT. The *G/D* ratio is a direct measure of the quality of a sample.

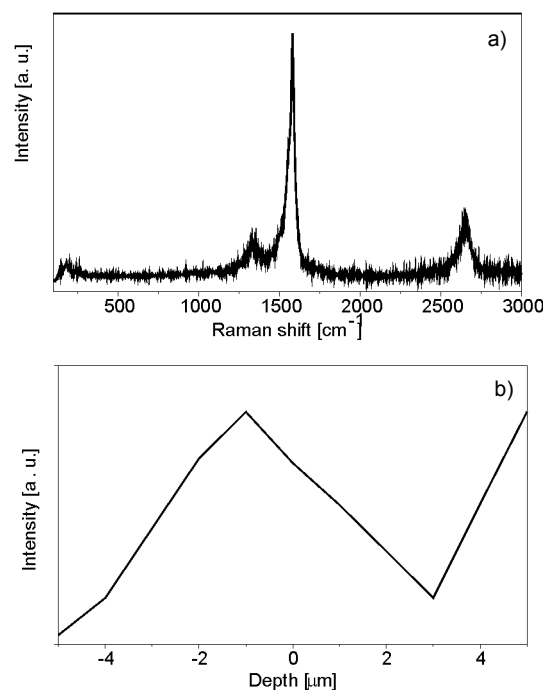


Fig. 6. Raman spectrum of SWCNT (a), and the depth profile of the G band in two dimensions

Mapping analysis is important to see the homogeneity of the sample and compare the different Raman features in the select area. The depth profile is useful beyond the standard spectra, to select how the Raman signal changes in respect to the depth of the sample.

References

- [1] DRESSELHAUS M.S., DRESSELHAUS G., SAITO R., JORIO A., *Phys. Rep.*, 409 (2005), 47.
- [2] JORIO A., PIMENTA M.A., FANTINI C., SOUZA M., SOUZA FILHO A.G., SAMSONIDZE GE.G., DRESSELHAUS G., DRESSELHAUS M.S., SAITO R., *Carbon*, 42 (2004), 1067.
- [3] KAVAN L., RAPTA P., DUNSCH L., BRONIKOWSKI M.J., WILLIS P., SMALLEY R.E., *J. Phys. Chem. B*, 105 (2001), 10764.
- [4] ALVAREZ L., RIGHI A., GUILLARD T., ROLS S., ANGLARET E., LAPLAZE D., SAUVAJOL J.-L., *Chem. Phys. Lett.*, 316 (2000), 186.
- [5] ASTAKHOVA T.YU., VINOGRADOV G.A., MENON M., *Russian Chem. Bull., Int. Ed.*, 52 (2003), 823.
- [6] DRESSELHAUS M.S., DRESSELHAUS G., JORIO A., SOUZA FILHO A.G., PIMENTA M.A., SAITO D.R., *Acc. Chem. Res.*, 35 (2002), 1070.
- [7] QIAN W., LIU T., WEI F., YUAN H., *Carbon*, 41 (2003), 1851.
- [8] TAKEDA N., MURAKOSHI K., *Anal Bioanal Chem.*, 388 (2007), 103.
- [9] DOORN S.K., HELLER D.A., BARONE P.W., USREY M.L., STRANO M.S., *Appl. Phys. A*, 78 (2004), 1147.

- [10] DRESSELHAUS M.S., DRESSELHAUS G., JORIO A., SOUZA FILHO A.G., SAITO R., *Carbon*, 40 (2002), 2043.
- [11] DRESSELHAUS M.S., JORIO A., SOUZA FILHO A.G., DRESSELHAUS G., SAITO R., *Physica B*, 323 (2002), 15.
- [12] ZHANG H.B., LIN G.D., ZHOU Z.H., DONG X., CHEN T., *Carbon*, 40 (2002), 2429.
- [13] ANTUNES E.F., LOBO A.O., CORAT E.J., TRAVA-AIROLDI V.J., MARTIN A.A., VERISSIMO C., *Carbon*, 44 (2006), 2202.
- [14] RITTER U., SCHARFF P., SIEGMUND C., DMYTRENKO O.P., KULISH N.P., PRYLUTSKYY YU.I., BELYI N.M., GUBANOV V.A., KOMAROVA L.I., LIZUNOVA S.V., POROSHIN V.G., SHLAPATSKAYA V.V., BERNAS H., *Carbon*, 44 (2006), 2694.
- [15] GRIMM D., GRÜNEIS A., KRAMBERGER C., RÜMMELI M., GEMMING T., BÜCHNER B., BARREIRO A., KUZMANY H., PFEIFFER R., PICHLER T., *Chem. Phys. Lett.*, 428 (2006), 416.
- [16] DOORN S.K., O'CONNELL M.J., ZHENG L., ZHU Y.T., HUANG S., LIU J., *Phys. Rev. Lett.*, 16802 (2005), 1.
- [17] KUZMANY H., BURGER B., THESS A., SMALLEY R.E., *Carbon*, 36 (1998), 709.
- [18] KÜRTI J., KUZMANY H., BURGER B., HULMAN M., WINTER J., KRESSE G., *Synth. Metals*, 103 (1999), 2508.
- [19] KUZMANY H., PLANK W., HULMAN M., KRAMBERGER C., GRÜNEIS A., PICHLER T., PETERLIK H., KATAURA H., ACHIBA Y., *Eur. Phys. J. B*, 22 (2001), 307.

Received 28 April 2007
Revised 16 February 2008